

FRACTURE PROCESS OF PM Ti6Al4V AT 20K IN PRESENCE OF IMPURITIES

L. Briottet¹, N. Scheer¹ and D. Guichard²

¹ CEA/Grenoble, DRT/DTEN, 17 rue des martyrs,
38054 Grenoble cedex 9, France

² SNECMA/Division Moteurs Fusée, Forêt de Vernon, BP802,
27208 cedex Vernon, France

ABSTRACT

PM Ti6Al4V is foreseen to manufacture rocket engine components with complex geometry. The major drawback related to this process is the potential presence of impurities mixed with the initial powder. At cryogenic temperature, some of these pollutions lead to a strong decrease of the material ductility. In order to validate the Ti6Al4V powder metallurgy route for critical engine components, it is necessary to understand and quantify the influence of such pollutions. Due to diffusion during the compaction cycle, several layers with different chemical and crystallographic properties are formed. In this paper, an analysis by SEM and TEM of these phases is presented. Moreover, mechanical tests at 20K, including interrupted tensile tests, allow to discriminate the worst potential defects and to propose several fracture processes depending on the initial impurity chemical composition.

KEYWORDS

Ti6Al4V, powder metallurgy, defects, fracture mechanisms

INTRODUCTION

The improvement of rocket engine efficiency necessitates components with an increasing complex geometry. For cryogenic applications, the α/β Ti6Al4V titanium alloy is used owing to its high strength, specific modulus and ductility at such temperatures. To achieve complex geometry, the powder metallurgy route is foreseen with the additional advantage that it provides a good homogeneity of the microstructure. However, a major drawback comes from the possible presence of impurities in the initial powder before compaction. These impurities can be introduced either during the melting operation, during powder production or during subsequent handling. Some defects can be quite large, typically 500 μm diameter including the diffusion affected volume, and lead to a strong decrease of the ductility of the material at low temperature (20K) under monotonic loading. The aim of this study is to investigate the effect of various defects on the ductility as well as to understand the failure mechanisms in order to predict the rupture of a component under in-service conditions.

DEFECTS DESCRIPTION

The Ti6Al4V titanium alloy, widely used in aeronautic and astronautic industries, has the following composition (wt %) : Al 6, V 4, Ti bal. The powder metallurgy alloy microstructure consists of α (hcp) grains with two morphologies, globular or lath shape, embedded in a β (bcc) phase (~10% volume fraction). The potential impurities likely to be found are the following ones (including the composition of the principal elements in wt %) : In718 (Cr 19, Fe 18, Nb 5, Mo 3, Ni bal.), In625 (Cr 20, Mo 8, Nb 3.5, Ni bal.), Astroloy (Cr 15, Mo 5, Al 4, Ti 3.5, Co 1.5, Ni bal.), FeNi (Fe 70, Ni 30), Stellite 21 (Cr 26, Mo 5.5, Ni 2.5, S, 1, C 0.25, Co bal.). After the compaction HIP cycle, followed by a classical heat treatment in order to control the titanium alloy microstructure, the defects present several layers due to cross-diffusion of chemical elements as shown in Figure 1. In these micrographs, displaying the chemical contrast (BSE), the surrounding laths correspond to Ti6Al4V material still affected by diffusion and not yet to the bulk material. By changing the contrast in the bright centre of the defects, more layers can be observed. SEM chemical analysis shows that for the three Ni base alloys analysed, the composition of the initial powder particle completely vanishes, mainly due do Ti diffusion from the matrix and Ni diffusion to the matrix. In the Co base alloy, a similar phenomena is observed with more Ti and a lack of Co in the centre. By contrast, the centre of the FeNi defect remains almost unaffected by diffusion (less than 2% Ti is observed). Of course, these considerations are linked to the unknown size of the initial defect particle of powder, which is at least the diameter of the central layer after compaction.

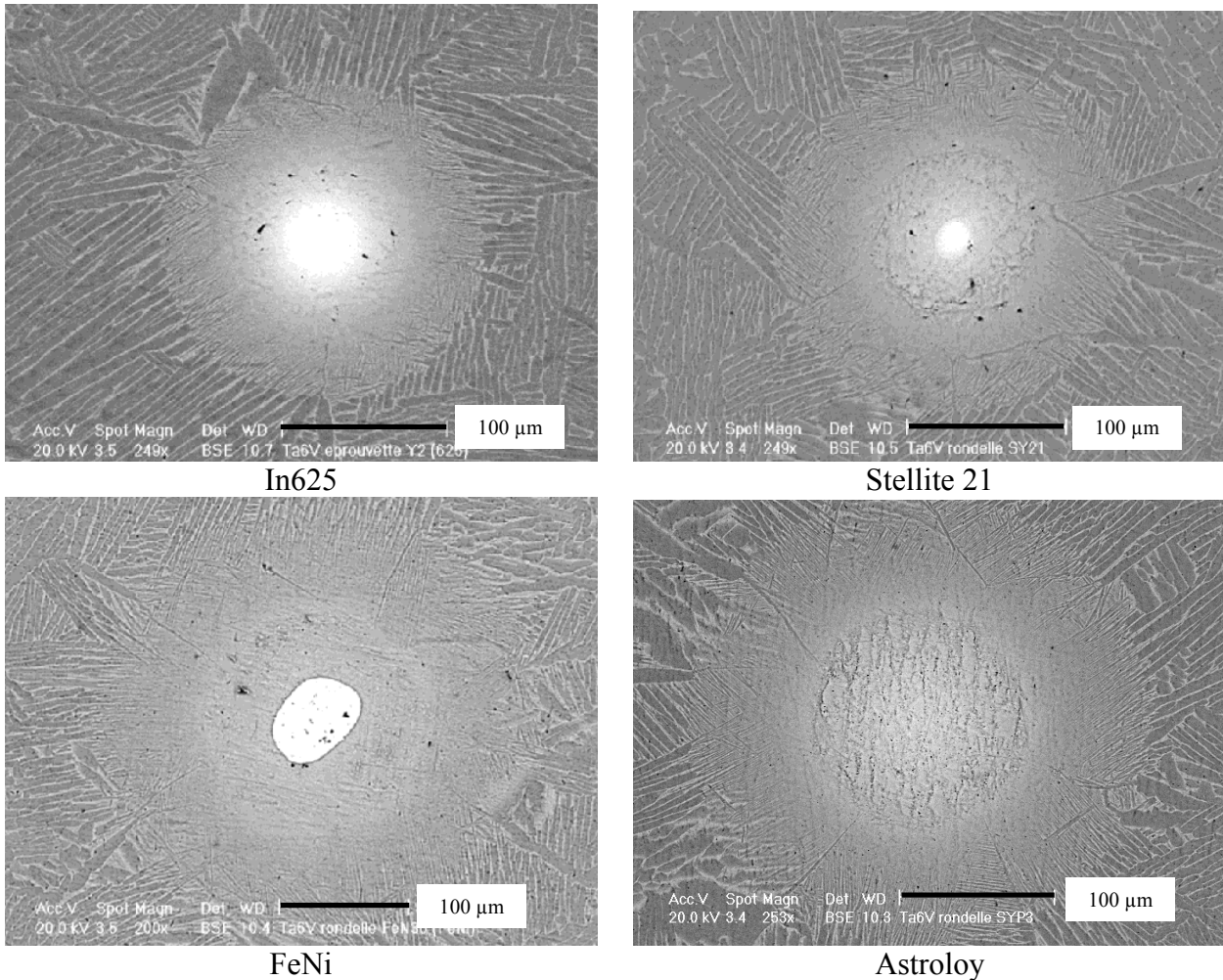


Figure 1: Overall aspect of the pollutions

To identify the phases responsible for damage initiation, thin foils have been prepared with care in a In718 pollution for TEM observations (Figure 2). The centre of the pollution is composed of a bcc phase corresponding to Ti β rich in Cr, and a Ti₂Ni fcc phase with grains of a few μ m. The surrounding large layer

consists in large $Ti\beta$ grains : a single grain through the whole thickness. The In625 defects are similar to the In718 ones (the main chemical difference is due to the amount of Fe in In718).

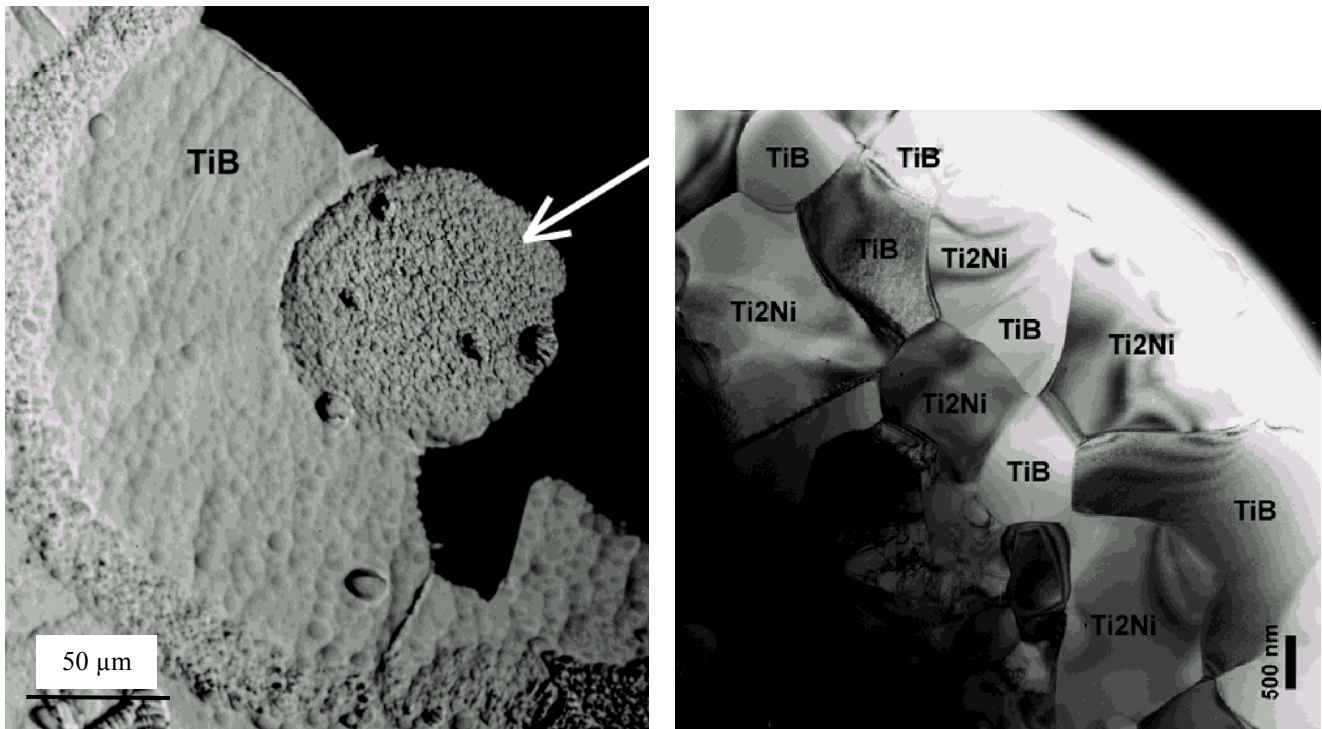


Figure 2: SEM (left) and TEM (right) observation of a In718 pollution in the Ti6Al4V matrix

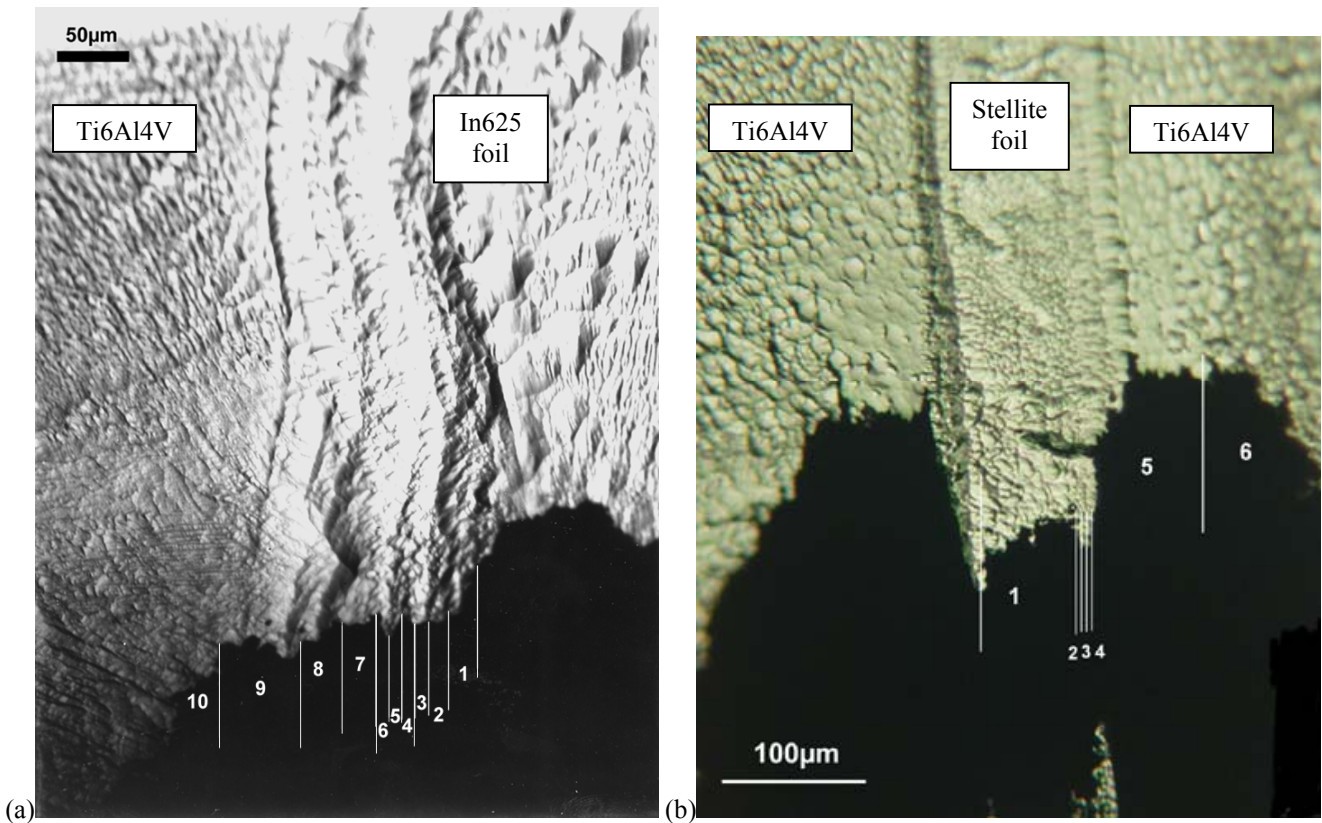


Figure 3: Plane defect (a) In625 foil (b) Stellite foil

Due to the heterogeneous thinning of the thin foil, it was not possible to analyse all the layers observed on spherical defects (Figure 2). Thus, flat defects have been performed by introducing a In625 or a Stellite foil (~100 μm thick) in the Ti6Al4V before compaction. With this defect geometry, thinning crosses the whole layers as seen in Figure 3. All the different phases can here be addressed by TEM analysis. However, the

results have to be handle with care since the diffusion process is not the same for a spherical powder than for a foil. Indeed, some phases observed for one type of geometry may not exist for the second type.

For the Stellite defect a large Ti β layer is also identified. Moreover, in the small layers close to the defect centre several intermetallics are observed : TiCo, Ti₂Co and CoCr.

MECHANICAL TESTS

In order to analyse the effect of such impurities on the material ductility, tensile tests have been performed at 20K on blocks compacted from voluntarily polluted Ti6Al4V powders. After the compaction cycle, the main pollutions have been localised by X-ray NDE. Smooth and flat tensile specimens have then been machined to settle the impurities in their gage length. A low strain-rate has been imposed in order to avoid thermo-mechanical instabilities likely to occur in this material [1] at that temperature. The main results are displayed in Table 1 showing total elongation in presence of large enough impurities :

TABLE 1
TENSILE RESULTS AT 20K : TOTAL ELONGATION FOR EACH POLLUTION

pollution	no	Astroloy	In625	Stellite	FeNi	In718
TE (%)	~15	~15	~8	~5	~5	~2

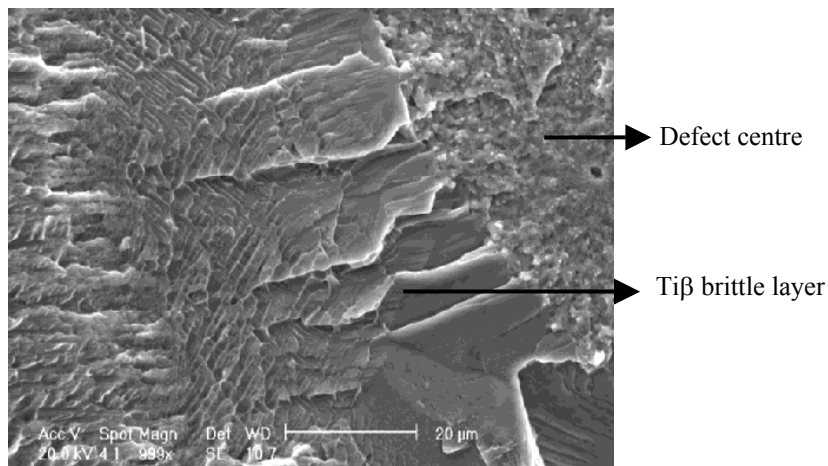


Figure 4: Fracture surface on a In625 pollution at 20K

As can be seen in this Table, Astroloy has no dramatic effect on ductility. By contrast, the other defects lead to a strong decrease of total elongation. Stellite, FeNi and In718 are the more dangerous defects. Tensile tests performed at several temperatures up to 293K emphasize the strong temperature influence on the defect/damage interaction : above 50K, no decrease of ductility is observed whatever the impurity present in the Ti6Al4V blocks.

A fractography of a specimen tested at 20K and containing a In625 pollution is displayed in Figure 4. Some of the layers observed previously by SEM and TEM examinations (Figures 1 and 2) can clearly be identified in this micrograph : the polyphase centre with a rough aspect and the surrounding Ti β layer known to be brittle as confirmed on this Figure. The outermost layers exhibit a more classical ductile aspect.

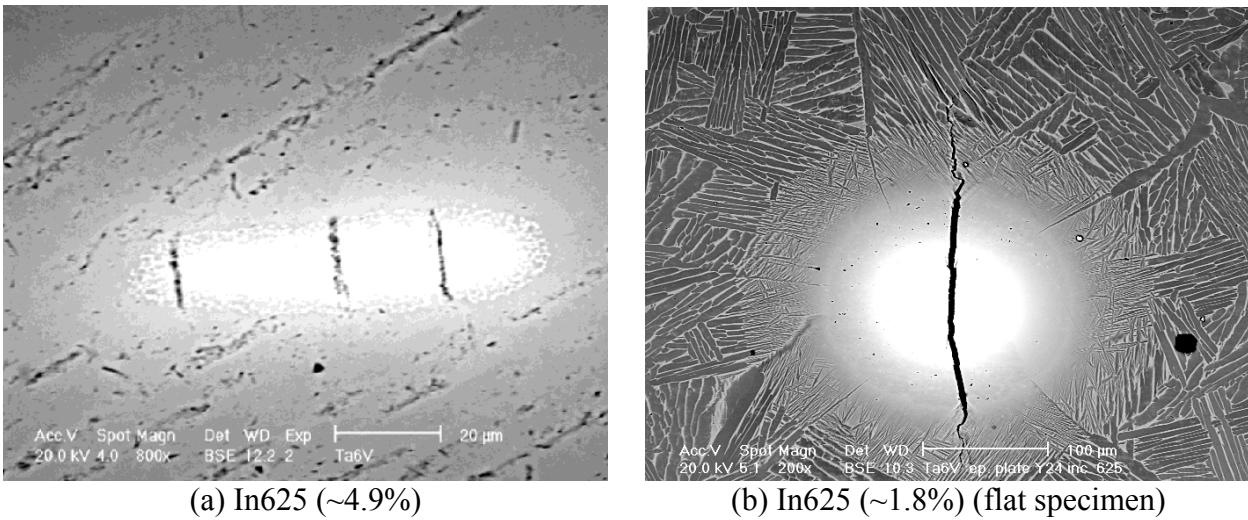


Figure 5: Different stages of damage on In625 pollutions (horizontal loading direction)

Interrupted tests have been performed to analyse damage initiation in presence of such impurities. In Figure 5, different stages of the crack evolution are presented for a In625 pollution. The crack initiates in the centre (Figure 5a) of the defect probably composed of the following brittle phases : $Ti\beta$ and Ti_2Ni (as seen in the In718 TEM analysis). Moreover, due to the chemical compositions observed, a Laves phase Cr_2Ti [2] is also expected depending on the diameter of the initial powder. The crack then propagates first in a brittle fashion through the $Ti\beta$ layer and finally reaches the unaffected Ti6Al4V material (Figure 5b) where it grows between the α laths. From the very beginning of the damage process, the crack is observed perpendicular to the loading direction. Due to the similarities between In625 and In718 chemical composition and fractographies, the same type of propagation is expected in In718.

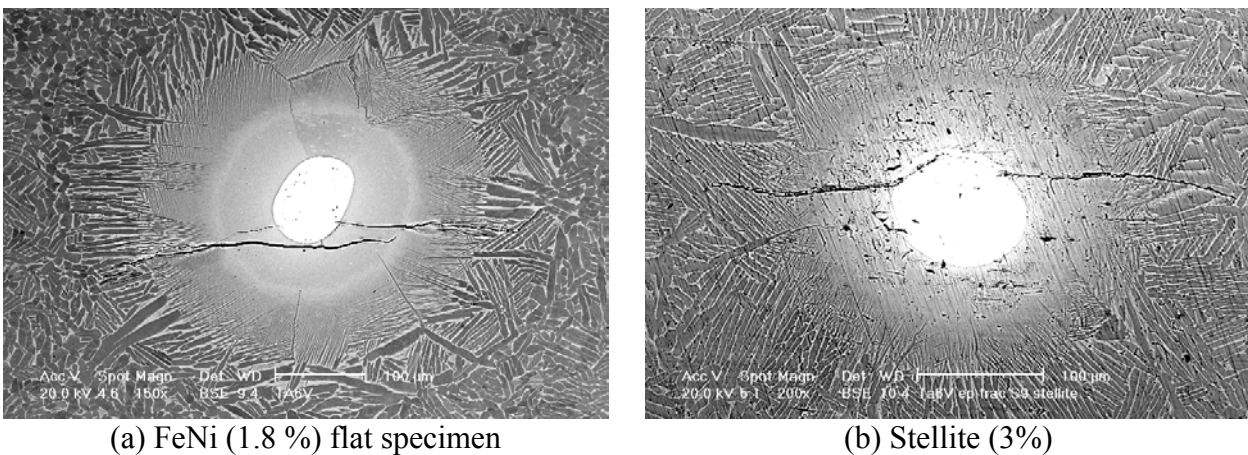


Figure 6: Damage initiation in FeNi (left) and Stellite (right) – (vertical loading direction)

By contrast, for FeNi (Figure 6a) and Stellite (Figure 6b), the crack never propagates through the defect centre. In both cases, the $Ti\beta$ brittle layer is broken perpendicularly to the loading direction and the crack pass round the centre.

DISCUSSION

The main conclusion derived from these experiments are presented in Table 2. Interrupted tests at the Ti6Al4V yield stress showed that in the case of FeNi and Stellite, a crack is already present at that stress level. Due to the low ductility observed in presence of In718 defects, it is expected that crack initiation occurs also for an overall stress close to the yield stress. By contrast, in the case of In625, crack initiation is observed after the yield stress.

TABLE 2
MAIN CONCLUSIONS ON THE DEFECTS INFLUENCE ON DAMAGE

pollution		astroloy	In625	FeNi	Stellite	In718
Induced damage	Initiation	-	$\sigma > YS$	$\sigma \leq YS$	$\sigma \leq YS$	$\sigma \leq YS ?$
	Min. defect radius	-	$R > 100\mu\text{m}$		$R > 50\mu\text{m}$	
	TE decrease	-	small	strong	strong	strong

By analysing many samples of In625 and Stellite, a minimum size of the defect centre necessary to induce accelerated damage has been defined. Due to diffusion, the size of the initial defect particle was certainly greater. However, it appears that a pollution of Stellite roughly twice smaller than a In625 one is sufficient to induce damage.

From the above results, we can propose the following fracture processes for the several types of impurities. For In718 and In625, the critical stress for cleavage is first reached in one of the intermetallic compounds present in the central part of the defect. The small grains as well as the polyphase microstructure explain the rough aspect observed on the fractography. In a second step, due to stress concentration at the crack tip and increase of the overall stress, the critical stress in the $Ti\beta$ is reached leading to the brittle propagation seen in Figure 4. In718 is found more dangerous than In625 probably due to a particular intermetallic with a lower cleavage stress. The damage stages of FeNi and Stellite are quite different. From the micrographs performed on interrupted tests, it appears that the first stage corresponds to the brittle rupture of the $Ti\beta$ layer. The crack then propagates towards the centre following the interface between the centre and the surrounding layer.

This mechanism can explain the effect of temperature by the low sensitivity of the cleavage critical stress σ_c with temperature. If σ_c is considered constant with T, an increase of the testing temperature leads to a decrease of the stresses magnitude in the whole defects. Above 50K, the damage mechanism in the unaffected Ti6Al4V is initiated before cleavage in any of the brittle layers of the defects.

The next step is to quantify the critical stress of the observed brittle layers since in the literature these intermetallics compounds have only been studied at high temperatures.

ACKNOWLEDGEMENTS

The authors are thankful to the Centre National d'Etudes Spatiales for partial financial support of this work, and to I. Chu and S. Pachot for SEM and TEM contributions.

REFERENCES

- [1] Ambard, A., Guétaz, L., Briottet, L., and Guichard, D. (1999) IN : *Proc. Of the 9th World Conference on Titanium*, pp. 608-615, Saint Petersburg, Russia.
- [2] Van Beek, J.A., Kodentsov, A.A. and Van Loo, F.J.J. (1998) *J. Alloys Comp.* 270, 218.